

New Type 2 Copper–Cysteinate Proteins. Copper Site Histidine-to-Cysteine Mutants of Yeast Copper–Zinc Superoxide Dismutase

Yi Lu,^{†,‡} James A. Roe,[§] Christopher J. Bender,^{||} Jack Peisach,^{||} Lucia Banci,[⊥] Ivano Bertini,[⊥] Edith B. Gralla,[†] and Joan Selverstone Valentine^{*,†}

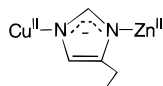
Department of Chemistry and Biochemistry, University of California, Los Angeles, Los Angeles, California 90095, Department of Molecular Pharmacology, Albert Einstein College of Medicine of Yeshiva University, Bronx, New York 10461, Department of Chemistry and Biochemistry, Loyola Marymount University, Los Angeles, California 90045, and Department of Chemistry, University of Florence, Florence, Italy

Received October 13, 1995[⊗]

Preparation and characterization of two new site-directed mutant copper–zinc superoxide dismutase proteins from *Saccharomyces cerevisiae*, i.e., His46Cys (H46C) and His120Cys (H120C), in which individual histidyl ligands in the copper-binding site were replaced by cysteine, are reported here. These two mutant CuZnSOD proteins may be described as type 2 (or normal) rather than type 1 (or blue) copper–cysteinate proteins and are characterized by their yellow rather than blue color, resulting from intense copper-to-sulfur charge transfer bands around 400 nm, their type 2 EPR spectra, with large rather than small nuclear hyperfine interactions, and their characteristic type 2 d–d electronic absorption spectra. An interesting difference between these two copper site His-to-Cys mutations is that the imidazolate bridge between the two metal sites that is characteristic of the wild-type protein remains intact in the case of the H46C mutant but is not present in the case of the H120C mutant.

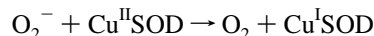
Introduction

Copper–zinc superoxide dismutase (CuZnSOD)¹ is a dimeric enzyme with a Cu(II) ion ligated to four histidines and a Zn(II) ion ligated to three histidines and a single aspartate in each of its two identical subunits.^{2–4} A unique feature of this enzyme is that the two metal binding sites share a common ligand, the bridging histidine, which binds to both the Cu(II) and the Zn(II) sites through an imidazolate side chain.



Mechanistic studies of CuZnSOD have focused on reactions of the substrate, superoxide anion, with both the oxidized and reduced enzyme. Of particular interest are the roles various amino acid residues play in providing electrostatic guidance to the superoxide anion as it is drawn into the active site channel leading to the copper ion, the role of anionic inhibitors of the enzyme, and the details of the reaction of superoxide with the

copper ion in either its oxidized or reduced state.^{2–4}



Another area of interest is the role of the zinc–imidazolate ligand bound to copper(II) in the oxidized state of the enzyme (see Figure 1). This type of ligation is unique to CuZnSOD, and yet its functional significance is largely unknown.

Recently we have prepared and characterized site-directed mutants of CuZnSOD from the yeast *Saccharomyces cerevisiae* in which histidyl ligands in the copper and zinc metal-binding sites have been replaced by cysteine. We have already reported some of our results concerning zinc site His-to-Cys mutations and have described the characterization of a new type 1 (blue) copper site prepared in this fashion by substitution of Cu(II) for Zn(II) in the mutated zinc site.^{5–8} We now report the characterization of two copper site His-to-Cys mutants, i.e., His46Cys (H46C) and His120Cys (H120C) (see Figure 1) in which the newly introduced cysteine ligands bind to Cu(II) centers and yet the new copper–cysteinate proteins do not have the characteristics of type 1 centers. An interesting difference between the two copper site His-to-Cys mutant proteins is that the imidazolate bridge between the two metal sites remains intact in the H46C mutant but is not present in the H120C mutant. Analysis of the X-ray crystal structures of CuZnSOD proteins suggests an explanation for these results, i.e. that the H120C

[†] University of California, Los Angeles.

[‡] Current address: Department of Chemistry, University of Illinois, Urbana, IL 61801.

[§] Loyola Marymount University.

^{||} Albert Einstein College of Medicine.

[⊥] University of Florence.

[⊗] Abstract published in *Advance ACS Abstracts*, January 15, 1996.

- (1) Abbreviations: M₂M'₂SOD, M- and M'-substituted superoxide dismutase with M in the copper site and M' in the zinc site (an E in the above derivatives represents an empty site); UV–vis, electronic absorption spectroscopy in the ultraviolet and visible range; RR, resonance Raman; EPR, electron paramagnetic resonance; ESEEM, electron spin echo envelope modulation; NMR, nuclear magnetic resonance.
- (2) Valentine, J. S.; Pantoliano, M. W. In *Copper Proteins*; Spiro, T. G., Ed.; John Wiley and Sons, Inc.: New York, 1981; pp 291–358.
- (3) Bertini, I.; Banci, L.; Piccioli, M. *Coord. Chem. Rev.* **1990**, *100*, 67–103.
- (4) Bannister, J. V.; Bannister, W. H.; Rotilio, G. *CRC Crit. Rev. Biochem.* **1987**, *22*, 111–180.

- (5) Han, J.; Loehr, T. M.; Lu, Y.; Valentine, J. S.; Averill, B. A.; Sanders-Loehr, J. *J. Am. Chem. Soc.* **1993**, *115*, 4256–4263.
- (6) Lu, Y.; Gralla, E. B.; Roe, J. A.; Valentine, J. S. *J. Am. Chem. Soc.* **1992**, *114*, 3560–3562.
- (7) Lu, Y.; Gralla, E. B.; Valentine, J. S. In *Bioinorganic Chemistry of Copper*; Karlin, K. D., Tyeklár, Z., Eds.; Chapman & Hall: New York, 1993; pp 64–77.
- (8) Lu, Y.; LaCroix, L. B.; Lowery, M. D.; Solomon, E. I.; Bender, C. J.; Peisach, J.; Roe, J. A.; Gralla, E. B.; Valentine, J. S. *J. Am. Chem. Soc.* **1993**, *115*, 5907–5918.

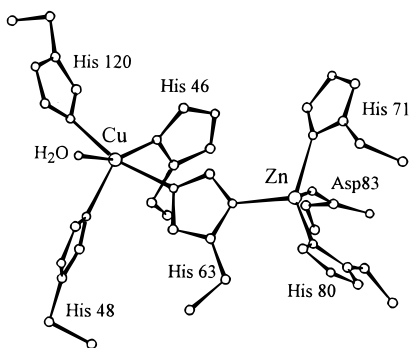


Figure 1. Metal binding sites of CuZnSOD from *S. cerevisiae*.

mutation causes the Cu(II) ion to be pulled away from the zinc-binding site so that the imidazolite bridge does not form. These results and our analysis are the subject of this report.

Experimental Section

Construction, expression, and purification of metal-binding mutants were carried out as described previously,^{8,9} using a 26-mer oligonucleotide for site-directed mutagenesis (5'-GAACGTGGGTTCTGCATTCATGAGTT for H46C and 5'-AGCGTCGTTATCTGCGCCGGC-CAAGA for H120C). Sample preparation and spectroscopic measurements (AA, UV-vis, EPR, and ESEEM) were also carried out as described previously.^{8,9} NMR spectra were obtained with a Bruker MSL 200 NMR spectrometer, operating at 200.13 MHz, using the MODEFT pulse sequence.¹⁰ In order to ensure the homogeneity of the sample when making the E₂Co₂ and the Cu₂Co₂ derivatives for NMR characterization, the NMR spectrum was measured after each addition of 0.5 equiv (per dimer) of Co²⁺ to either apoprotein (for E₂Co₂) or apoprotein already loaded with 2 equiv of Cu²⁺ (for Cu₂Co₂). The resulting NMR spectra displayed a set of signals that increased in intensity as the amount of metal ion added was increased. The increase of signals continued until the saturation of the site was reached (at 2 equiv), without displaying new signals, thus establishing that each of the samples (E₂Co₂ and Cu₂Co₂) was homogeneous. Throughout this paper, the stated numbers of equivalents of metal ions added to the protein are per protein dimer. The buffer was 100 mM sodium acetate, pH 5.5. The addition of metal ions and the measurement of spectra were carried out at ambient temperature except where otherwise specified.

Results

Electronic Absorption Spectroscopy. 1. Cu₂Cu₂ and Cu₂Zn₂ Derivatives. The UV-vis absorption spectra associated with the addition of Cu²⁺ alone (Figure 2) or addition of Zn²⁺ followed by Cu²⁺ (Figure 3) to recombinant WT, H46C, and H120C proteins were recorded. Table 1 contains a summary of the electronic absorption bands and tentative assignments for Cu₂E₂⁻, Cu₂Cu₂⁻ and Cu₂Zn₂⁻ derivatives of each. In the case of WT, the spectra were found to be similar to those observed previously for bovine CuZnSOD.^{8,11} When the first 2 equiv of Cu²⁺ was titrated into recombinant apo-WT protein (Figure 2Ab,Ac), a broad absorption, around 664 nm ($\epsilon = 156 \text{ M}^{-1} \text{ cm}^{-1}$), was observed. When the second 2 equiv of Cu²⁺ was added, another lower energy absorption around 810 nm ($\epsilon = 214 \text{ M}^{-1} \text{ cm}^{-1}$) appeared (data not shown). When Zn²⁺ was added prior to Cu²⁺ (Figure 3Ac,Ad), only a single band, around 670 nm ($\epsilon = 147 \text{ M}^{-1} \text{ cm}^{-1}$), was observed.

The UV-vis bands described above for the yeast protein were previously assigned for the analogous bovine CuZnSOD derivatives to the d-d transitions of Cu(II) in the two different metal

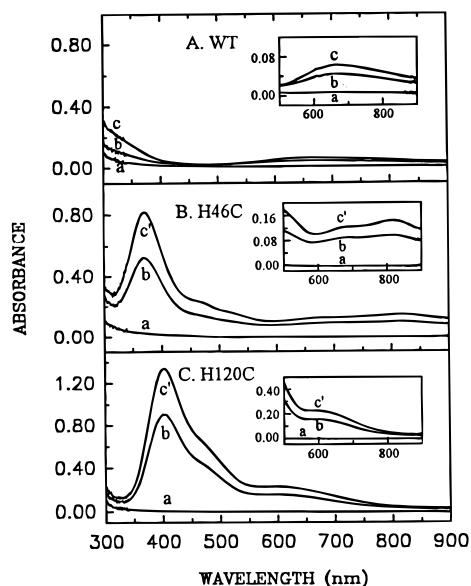


Figure 2. Electronic absorption spectra of the Cu₂E₂ derivatives of recombinant yeast wild type (WT) and the copper site mutant proteins H46C and H120C. Subunit concentrations of the protein samples were as follows: (A) WT, 0.40 mM; (B) H46C, 0.48 mM; (C) H120C, 0.46 mM. The amount of Cu²⁺ added (per dimer) was as follows: (a) apoprotein; (b) apoprotein plus 1.0 equiv Cu²⁺; (c) apoprotein plus 2.0 equiv of Cu²⁺; (c') apoprotein plus 1.6 equiv of Cu²⁺.¹³

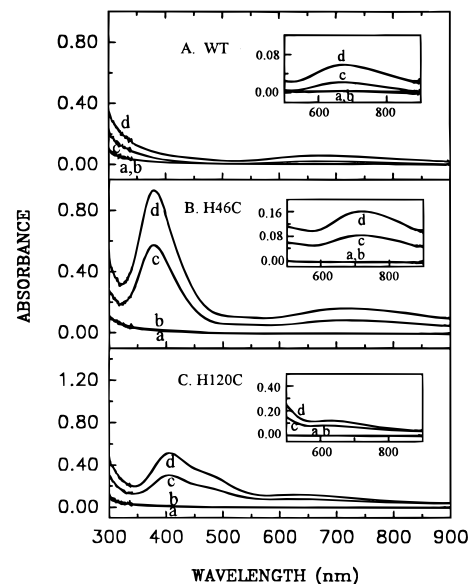


Figure 3. Electronic absorption spectra of the Cu₂Zn₂ derivatives. Subunit concentrations of the protein samples were the same as in Figure 2. The amount of metal added (per dimer) was as follows: (a) apoprotein; (b) apoprotein plus 2.0 equiv of Zn²⁺; (c) apoprotein plus 2.0 equiv of Zn²⁺ and plus 1.0 equiv of Cu²⁺; (d) apoprotein plus 2.0 equiv of Zn²⁺ and plus 2.0 equiv of Cu²⁺.

binding sites, the higher energy band being assigned to Cu(II) in the roughly tetragonal copper site and the lower energy band to Cu(II) in the approximately tetrahedral zinc site, by analogy to spectra of copper coordination complexes of known geometries.¹¹ For Cu²⁺ added to yeast apo-WT protein as described above, we similarly assign the band at 664 nm to Cu(II) in the copper site and the band at 810 nm to copper in the zinc site. We interpret the observation that the 810 nm band did not appear when 2 equiv of Zn²⁺ was added prior to the addition of Cu²⁺ as indicating that Zn(II) bound to the zinc site was not readily displaced by subsequent addition of Cu²⁺. Thus only the band due to the Cu²⁺ in the copper site (670 nm) was observed. The

(9) Lu, Y. Ph.D. Dissertation, UCLA, Los Angeles, CA, 1992.

(10) Hochmann, J.; Kellerhals, H. P. *J. Magn. Reson.* **1980**, *38*, 23–39.

(11) Pantoliano, M. W.; Valentine, J. S.; Nafie, L. A. *J. Am. Chem. Soc.* **1982**, *104*, 6310–6317.

Table 1. Electronic Absorption Data for Cu₂E₂, Cu₂Cu₂, and Cu₂Zn₂ Derivatives of Yeast Recombinant Wild Type and the Copper Site Mutants H46C and H120C^a

| | Apo | Cu ₂ E ₂ | Cu ₂ Cu ₂ | Cu ₂ Zn ₂ | assignment |
|-------|------------|--------------------------------|---------------------------------|---------------------------------|------------------------|
| WT | 258 (2930) | 258 (4650) | 258 (8240) | 258 (6710) | ImH→Cu CT |
| | 284 (2360) | 284 (3320) | 284 (5710) | 284 (3710) | ImH→Cu CT |
| | | 330 sh (519) | 340 sh (1610) | 340 sh (419) | ImH→Cu CT |
| | | | 420 sh (272) | 420 sh (134) | Im ⁻ →Cu CT |
| | | | 664 (192) | 670 (147) | Cu d-d |
| | | | 810 (214) | | Cu d-d |
| H46C | 258 (2660) | 258 (5600) | 258 (10,000) | 258 (6570) | ImH→Cu CT |
| | 284 (2380) | 284 (4130) | 284 (4400) | 284 (4050) | ImH→Cu CT |
| | | 371 (2130) | 410 (520) | 379 (1940) | Cys→Cu CT |
| | | 470 sh (596) | | | ? |
| | | 525 sh (406) | | | ? |
| | | 667 (315) | 671 (150) | 700 (333) | Cu d-d |
| | 810 (372) | | | Cu d-d | |
| H120C | 258 (2310) | 258 (4500) | 258 (12,000) | 258 (6810) | ImH→Cu CT |
| | 284 (2090) | 284 (3250) | 284 (5100) | 284 (4470) | ImH→Cu CT |
| | | 402 (3640) | 403 (1000) | 406 (1250) | Cys→Cu CT |
| | | 470 sh (1740) | 470 sh (660) | 470 sh (710) | ? |
| | | 620 (600) | 677 (310) | 640 (259) | ? |
| | | | | | ? |

^a Positions in nanometers (nm); extinction coefficient, in units of M⁻¹ cm⁻¹, based on subunit concentration of the protein are in parentheses; sh, shoulder.

energy of the d-d transition from Cu(II) in yeast WT Cu₂Zn₂-SOD (670 nm) is slightly lower than that from Cu(II) in yeast WT Cu₂E₂SOD (664 nm), suggesting that the presence of Zn(II) in Cu₂Zn₂SOD may cause the environment of the Cu(II) center to be slightly more distorted toward tetrahedral than it is in Cu₂E₂SOD. A similar finding is reported for a mononuclear Co(II) derivative of hemocyanin, i.e., the addition of a single Cu²⁺ to form a mixed metal, binuclear center alters the optical properties of the initially bound Co(II), signifying an increase in the tetrahedral character of the Co(II)-binding site.¹²

By contrast to yeast apo-WT protein, which binds Cu²⁺ selectively to the copper site prior to binding to the zinc site, addition of up to 1.6 equiv per dimer of Cu²⁺ to apo-H46C causes the absorption bands due to Cu(II) in the copper site (667 nm) and in the zinc site (810 nm) to appear simultaneously (Figure 2Bb,Bc').¹³ Nevertheless, addition of 2 equiv of Zn²⁺ prior to the addition of Cu²⁺ resulted in the appearance of only one d-d transition around 700 nm (Figure 3Bd), indicating that Zn(II) blocked the zinc site and Cu(II) was bound only to the copper site, as in WT. In spite of the fact that the H46C mutation clearly results in some difference in the relative affinities of the copper and zinc sites for Cu²⁺, the similarity of the d-d regions (both the positions and the intensities) of the Cu₂Zn₂- and copper-substituted derivatives of WT and H46C indicates that the geometries of the copper and the zinc sites are not greatly changed by the mutation.

Whereas the d-d regions of the UV-vis spectra of copper-containing derivatives of WT and H46C are very similar, there is a dramatic difference in the higher energy region of the spectrum. A new, strong absorption band appears at λ_{max} = 371 nm (ε = 2130 M⁻¹ cm⁻¹) for H46C that is not present for WT (compare Figure 2Bc' with 2Ac and Figure 3Bd with 3Ad). The fact that similar absorption bands near 370 nm were present whether or not the zinc site was blocked with Zn(II) indicates that these bands can be attributed to the Cu(II) in the copper site, and we assign them as sulfur-to-Cu(II) charge transfer transitions (Table 1) on the basis of their high extinction coefficients.¹⁴

The spectra associated with adding Cu²⁺ alone (Figure 2Cb,-Cc') or adding Zn²⁺ followed by Cu²⁺ (Figure 3Cc,Cd) to apo-H120C resulted in spectroscopic changes relative to WT that are similar to those observed for the H46C mutant, but analysis of the d-d transition region of the spectrum is complicated by overlapping intensity due to the charge transfer bands, which trail off to lower energy. It is interesting to note that the extinction coefficient of the sulfur-to-copper charge transfer band in derivatives of H120C varies depending on whether or not the zinc site is occupied and, when occupied, on the identity of the metal ion bound (compare Figures 2Cc', 3Cd, and 4Cf).

2. E₂Co₂ and Cu₂Co₂ Derivatives. The UV-vis spectra observed after addition of Co²⁺ followed by addition of Cu²⁺ to apo-WT, apo-H46C and apo-H120C are given in Figure 4. The recombinant apo-WT protein showed behavior identical to that observed previously for the native protein¹⁵ in that apo-WT was found to bind only 2 equiv of Co²⁺ (Figure 4Ac) in acetate buffer, pH 5.5, and addition of a third equivalent of Co²⁺ caused little change in the spectrum (Figure 4Ad). The resulting three absorption bands (ε_{537nm} = 340 M⁻¹ cm⁻¹, ε_{566nm} = 450 M⁻¹ cm⁻¹, ε_{584nm} = 460 M⁻¹ cm⁻¹) are typical of d-d transitions for Co²⁺ in a tetrahedral site.¹⁶ When 2 equiv Cu²⁺ were then added to E₂Co₂, a band around 670 nm was observed (Figure 4Af), consistent with binding of Cu²⁺ to the copper site to give the Cu₂Co₂ derivative.

Closer inspection of the d-d absorption regions of E₂Co₂- and Cu₂Co₂-WT reveals shifts in the positions of the three absorption bands of Co(II) in the zinc site when the protein binds Cu²⁺. These changes can be seen more clearly after subtracting the Cu₂Zn₂SOD spectrum from that of Cu₂Co₂SOD to eliminate the contribution from Cu(II) d-d transitions in that region (Figure 5A). After addition of Cu²⁺, the lowest energy band shifted from 584 to 596 nm and the next higher energy band shifted from 566 to 568 nm. The highest energy band (537 nm) barely shifted. Similar changes were previously observed by Banci et al.¹⁷ in the analogous derivatives of bovine CuZnSOD, and the changes were attributed to the influence of

(12) Bubacco, L.; Magliozzo, R. S.; Beltramini, M.; Salvato, B.; Peisach, J. *Biochemistry* **1992**, *31*, 9294-9303.

(13) When >1.6 equiv of Cu²⁺ is added to apo-H46C under these conditions, the intensity of the 371 nm band is observed to diminish. When 2.0 equiv of Zn²⁺ is added first, the full 2.0 equiv of Cu²⁺ may then be added without loss of intensity of the 371 nm band.

(14) Lever, A. B. P. *Inorganic Electronic Spectroscopy*; Elsevier: New York, 1984.

(15) Ming, L.-J.; Banci, L.; Luchinat, C.; Bertini, I.; Valentine, J. S. *Inorg. Chem.* **1988**, *27*, 728-733.

(16) Bertini, I.; Luchinat, C. *Adv. Inorg. Biochem.* **1984**, *6*, 71-111.

(17) Banci, L.; Bertini, I.; Luchinat, C.; Monnanni, R.; Scozzafava, A. *Inorg. Chem.* **1987**, *26*, 153-156.

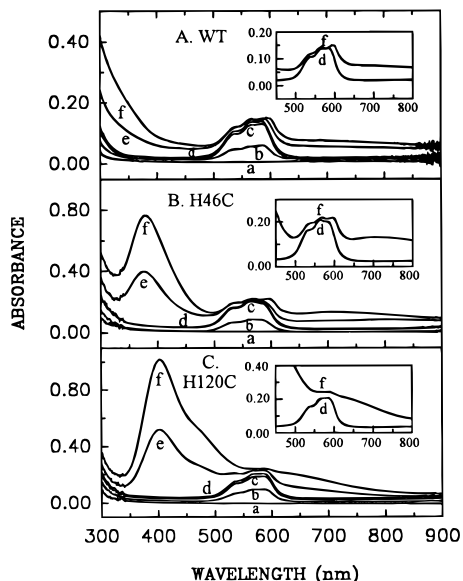


Figure 4. Electronic absorption spectra of the Cu_2Co_2 derivatives. Subunit concentrations of the protein samples were as follows: recombinant WT, 0.26 mM; H46C, 0.36 mM; H120C, 0.46 mM. The amount of Co^{2+} added (per dimer) was as follows: (a) apoprotein; (b) apoprotein plus 1.0 equiv of Co^{2+} ; (c) apoprotein plus 2.0 equiv Co^{2+} ; (d) apoprotein plus 3.0 equiv Co^{2+} ; (e) d plus 1.0 equiv of Cu^{2+} ; (f) d plus 2.0 equiv of Cu^{2+} .

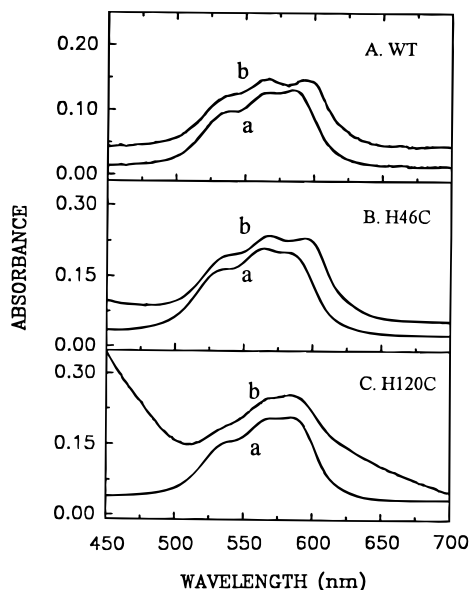


Figure 5. Electronic absorption spectra of Co(II) in the zinc site before and after addition of Cu^{2+} : (a) E_2Co_2 (see Figure 4Aa, 4Ba, 4Ca); (b) Cu_2Co_2 (see Figure 4Af, 4Bf, 4Cf) minus Cu_2Zn_2 (see Figure 3Ad, 3Bd, 3Cd).

$\text{Cu}(\text{II})$ in the copper site on the environment of $\text{Co}(\text{II})$ in the zinc site through the formation of the imidazolite bridge between the two metal ions. After careful comparisons of the optical spectra of several cobalt(II) derivatives of CuZnSOD , those authors concluded that addition of a metal into the copper site of the E_2Co_2 caused a shift of the three $\text{Co}(\text{II})$ d–d transitions *only* if the imidazolite bridge formed between the two metals. Otherwise, they concluded, the E_2Co_2 spectrum remained the same, even when the copper site was occupied by a metal ion.¹⁷

Just as with apo-WT, only 2 equiv of Co^{2+} bind to apo-H46C (Figure 4Bc) and to apo-H120C (Figure 4Cc). In both cases, Co^{2+} ions bind to the zinc site, as indicated by optical spectra characteristic of tetrahedrally coordinated Co^{2+} . When 2 equiv of Cu^{2+} was titrated into these E_2Co_2 derivatives, new charge

transfer bands around 400 nm were observed (Figure 4Bf and Figure 4Cf), which are similar to the charge transfer bands of the Cu_2Zn_2 and Cu_2Cu_2 derivatives of each protein, indicating that $\text{Cu}(\text{II})$ was likewise in the copper site, i.e., that the Cu_2Co_2 site had been formed.

It is interesting to note that changes in the $\text{Co}(\text{II})$ d–d spectrum of the H46C mutant upon binding Cu^{2+} to the E_2Co_2 derivative (Figure 5B) are very similar to those observed for WT and thus, following the analysis of Banci et al.,¹⁷ consistent with formation of an imidazolite bridge between $\text{Cu}(\text{II})$ and $\text{Co}(\text{II})$ in Cu_2Co_2 –H46C. By contrast, the observation that the d–d region of E_2Co_2 –H120C is unchanged when Cu^{2+} is added to form Cu_2Co_2 –H120 (Figure 5C) suggests that an imidazolite bridge between $\text{Cu}(\text{II})$ and $\text{Co}(\text{II})$ is not formed for that mutant. The conclusion that the imidazolite bridge characteristic of WT CuZnSOD might be preserved in Cu_2M_2 derivatives of H46C but not in similar derivatives of H120C was confirmed by ESEEM and NMR studies, as described below.

Electron Paramagnetic Resonance (EPR) Spectroscopy.

EPR spectra were obtained for Cu_2E_2 , Cu_2Cu_2 , and Cu_2Zn_2 derivatives of recombinant yeast WT CuZnSOD (Figures 6–8 and Table 2) and found to be very similar to spectra of the analogous derivatives of bovine CuZnSOD .² Addition of 2 equiv of Cu^{2+} to yeast apo-WT protein resulted in a Cu^{2+} EPR signal characteristic of a tetragonal site ($g_{\parallel} = 2.27$, $A_{\parallel} = 15.3 \times 10^{-3} \text{ cm}^{-1}$), consistent with our conclusion based on the UV–vis spectra that Cu^{2+} is bound to the copper site (i.e. Cu_2E_2). Addition of another 2 equiv of Cu^{2+} caused the EPR signal intensity to drop significantly, in a fashion similar to that observed previously for bovine CuZnSOD , suggesting that $\text{Cu}(\text{II})$ bound to the zinc site is antiferromagnetically coupled to the $\text{Cu}(\text{II})$ in the copper site through the imidazolite bridge.² This conclusion was confirmed by the observation of a half field EPR signal (Figure 7A), which is characteristic of an antiferromagnetically coupled $\text{Cu}(\text{II})$ pair.² When Cu^{2+} was added to apo-WT after overnight equilibration with 2 equiv of Zn^{2+} , a tetragonal Cu^{2+} EPR spectrum was also observed ($g_{\parallel} = 2.26$, $A_{\parallel} = 13.7 \times 10^{-3} \text{ cm}^{-1}$) (Figure 8A). However, the reduction of A_{\parallel} and increase of rhombicity of the EPR spectrum of $\text{Cu}_2\text{Zn}_2\text{SOD}$ relative to that of $\text{Cu}_2\text{E}_2\text{SOD}$ indicate that the geometry of $\text{Cu}(\text{II})$ in $\text{Cu}_2\text{Zn}_2\text{SOD}$ is more distorted from tetragonal than is that of $\text{Cu}_2\text{E}_2\text{SOD}$, as a consequence of occupancy of the zinc site by $\text{Zn}(\text{II})$. This conclusion is consistent with the shift in λ_{max} of the $\text{Cu}(\text{II})$ d–d transition from 664 nm to 670 nm (see discussion above and Table 1).

The magnetic coupling of the $\text{Cu}(\text{II})$ centers in the copper and zinc sites of Cu_2Cu_2 derivatives of CuZnSOD dramatically changes the nature of the EPR spectrum and thus makes similar analysis of the geometry of $\text{Cu}(\text{II})$ in the zinc site of this derivative impossible.² We therefore attempted to prepare the Ag_2Cu_2 derivative of yeast WT CuZnSOD in order to examine the EPR spectrum due to an individual $\text{Cu}(\text{II})$ ion in the zinc site. However, we failed to obtain a homogeneous sample of the Ag_2Cu_2 derivative of the yeast WT protein using the procedures that have been successful for bovine enzyme,¹⁸ for reasons that we do not understand. We therefore prepared a sample of bovine $\text{Ag}_2\text{Cu}_2\text{SOD}$ for comparison of its EPR spectrum with those of derivatives of H46C and H120C yeast CuZnSOD with $\text{Cu}(\text{II})$ in the zinc site (see below). Relative to the EPR spectrum of $\text{Cu}(\text{II})$ in the copper site of either the bovine or yeast proteins, the EPR spectrum of bovine $\text{Ag}_2\text{Cu}_2\text{SOD}$ (Figure 6Ad) had a smaller A_{\parallel} and increased rhombicity, typical of $\text{Cu}(\text{II})$ in a nonaxial site.¹¹ This observation is also

(18) Beem, K. M.; Richardson, D. C.; Rajagopalan, K. V. *Biochemistry* 1977, 16, 1930–1936.

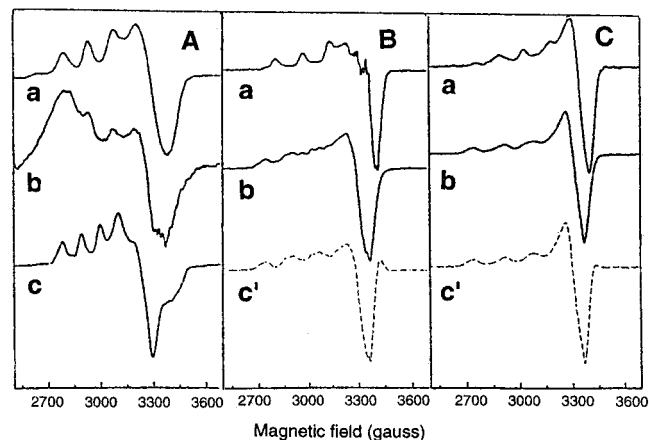


Figure 6. EPR spectra of copper derivatives of WT and the copper site mutant proteins H46C and H120C. Subunit concentrations of the samples: WT, 0.24 mM; H46C, 0.74 mM; H120C, 0.465 mM. Key: a, Cu_2E_2 ; b, Cu_2Cu_2 ; c, Ag_2Cu_2 derivative of bovine CuZnSOD ; c', b - a. Sample temperature: 90 K. Instrument settings: microwave frequency, 9.54 GHz; microwave power, 20 mW; modulation amplitude, 5 G; time constant, 640 ms.

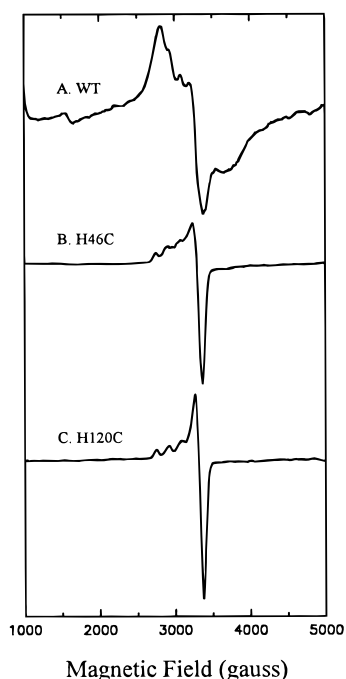


Figure 7. EPR spectra of the Cu_2Cu_2 derivatives including half-field region. Sample concentrations and instrument settings were the same as in Figure 6.

consistent with the electronic absorption spectra and suggests that the tetrahedral character of the zinc site is at least to some degree retained when it is occupied by copper.

Addition of 2 equiv of Cu^{2+} (per dimer) to apo-H46C also resulted in an EPR spectrum typical of a $\text{Cu}(\text{II})$ in a nearly tetragonal site (Figure 6Ba). However, the spectrum is more tetragonal than that of $\text{WT}-\text{Cu}_2\text{E}_2$, as evidenced by the nearly axial line shape and the larger A_{\parallel} ¹⁹ (for H46C, $A_{\parallel} = 17.9 \times 10^{-3} \text{ cm}^{-1}$, whereas, for wild type, $A_{\parallel} = 15.3 \times 10^{-3} \text{ cm}^{-1}$). Some superhyperfine splitting near g_{\perp} was also observed. The line shape of the spectrum is very similar to that of the CN^- adduct of the $\text{WT}-\text{Cu}_2\text{Zn}_2$ derivative, which has been interpreted as arising from a square planar $\text{Cu}(\text{II})$ coordination with the superhyperfine structure attributed to $\text{Cu}(\text{II})$ -nitrogen coupling.²⁰ The smaller g_{\parallel} for H46C relative to that of wild type, i.e. 2.23 vs 2.27, is also consistent with the binding of a

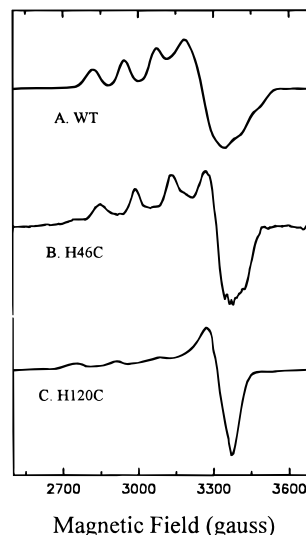


Figure 8. EPR spectra of the Cu_2Zn_2 derivatives. Subunit concentrations of the samples: WT, 1.35 mM; H46C, 0.50 mM; H120C, 0.46 mM. Sample temperature: 90 K. Instrument settings were the same as in Figure 6.

cysteinate ligand to the $\text{Cu}(\text{II})$ in place of an imidazole ligand.¹⁹ Addition of another 2 equiv of Cu^{2+} to Cu_2E_2 resulted in the EPR spectrum shown in Figure 6Bb. Unlike Cu_2Cu_2 -WT, there is no evidence for antiferromagnetic coupling (compare parts A and B of Figure 7). We take this spectrum as evidence that the imidazolate bridge between the two $\text{Cu}(\text{II})$ centers is not formed in that derivative. Subtraction of 40%²¹ of the Cu_2E_2 spectrum from the Cu_2Cu_2 spectrum resulted in the spectrum shown in Figure 6Bc', which is also that of Cu^{2+} in a tetragonal site. Assuming that the second 2 equiv of Cu^{2+} is bound to the zinc site of H46C as in WT, we conclude that the EPR spectrum due to $\text{Cu}(\text{II})$ in the zinc site of Cu_2Cu_2 -H46C (Figure 6Bc, $g_{\perp} = 2.07$, $g_{\parallel} = 2.30$, $A_{\parallel} = 17.4 \times 10^{-3} \text{ cm}^{-1}$) is dramatically different from the zinc site $\text{Cu}(\text{II})$ in bovine Ag_2Cu_2 -SOD (Figure 6Ac, $g_x = 2.01$, $g_y = 2.10$, $g_{\parallel} = 2.31$, $A_{\parallel} = 11.7 \times 10^{-3} \text{ cm}^{-1}$). However, it is very similar to that of the $\text{Cu}(\text{II})$ centers in lyophilized bovine Cu_2Cu_2 -SOD derivative ($g_{\perp} = 2.07$, $g_{\parallel} = 2.27$, $A_{\parallel} = 16.7 \times 10^{-3} \text{ cm}^{-1}$ for $\text{Cu}(\text{II})$ in both sites), where the imidazolate bridge between the two $\text{Cu}(\text{II})$ centers was shown to be broken as a consequence of the lyophilization.²² Therefore, the imidazolate bridge is not formed in Cu_2Cu_2 -H46C, and the zinc site is rearranged toward a more nearly tetragonal geometry.

The EPR spectrum of Cu_2Zn_2 -H46C is shown in Figure 8. Although the $\text{Cu}(\text{II})$ appears to be in a somewhat more tetragonal site in H46C than in WT, i.e., the g_{\parallel} feature is narrower, the EPR spectral changes observed in going from Cu_2E_2 -H46C to

(19) Peisach, J.; Blumberg, W. E. *Arch. Biochem. Biophys.* **1974**, *165*, 691-708.

(20) Rotilio, G.; Morpurgo, L.; Giovagnoli, C.; Calabrese, L.; Mondovì, B. *Biochemistry* **1972**, *11*, 2187-2192.

(21) Subtracting 40% rather than 100% of the Cu_2E_2 spectrum from that of Cu_2Cu_2 gave the best separation of the Cu_2E_2 signal from the new signal resulting from addition of the second 2 equiv of Cu^{2+} . Possible explanations are as follows: (1) the copper site may not have been saturated since the affinity of that site for Cu^{2+} is less when zinc is not present in the zinc site; (2) the line shape was changed due to a small shift in the geometry of $\text{Cu}(\text{II})$ in the copper site when $\text{Cu}(\text{II})$ goes into the zinc site, as evidenced by the disappearance of the hyperfine splitting in the EPR spectrum; (3) tuning the EPR instrument to maximize the signal-to-noise ratio resulted in apparent signal intensities for the different spectra that were not strictly proportional to the copper ion concentrations.

(22) Strothkamp, K. G.; Lippard, S. J. *J. Am. Chem. Soc.* **1982**, *104*, 852-853.

Table 2. EPR Parameters of Cu(II) Derivatives of Recombinant Yeast Wild Type and the Copper Site Mutants (H46C and H120C)

| | Cu ₂ E ₂ | | | Cu ₂ Cu ₂ minus Cu ₂ E ₂ | | | Cu ₂ Zn ₂ | | |
|--|--------------------------------|----------------|--|--|----------------|--|--|----------------|--|
| | g _⊥ | g _∥ | A _∥ (10 ³ cm ⁻¹) | g _⊥ | g _∥ | A _∥ (10 ³ cm ⁻¹) | g _⊥ | g _∥ | A _∥ (10 ³ cm ⁻¹) |
| recombinant wt | 2.07 | 2.27 | 15.3 | | | | g _x = 2.01 g _y = 2.10 | 2.26 | 13.7 |
| lyophilized bovine CuZnSOD ^a | 2.07 | 2.27 | 16.7 | 2.07 | 2.27 | 16.7 | 2.06 | 2.26 | 15.0 |
| H46C | 2.02 | 2.23 | 17.9 | 2.07 | 2.30 | 17.4 | g _x = 2.01 g _y = 2.06 | 2.23 | 15.1 |
| H120C | 2.04 | 2.20 | 15.8 | 2.06 | 2.27 | 17.0 | 2.05 | 2.27 | 17.5 |

^a Reference 22.

Cu₂Zn₂–H46C are quite similar to the changes occurring in the corresponding WT derivatives (see Table 2 for a comparison).

Addition of Cu²⁺ to apo-H120C to yield Cu₂E₂–H120C (Figure 6Ca) and Cu₂Cu₂–H120C (Figure 6Cb) resulted in spectral changes similar to those observed for the H46C mutant protein. In fact, subtraction of 40% of the EPR spectrum of Cu₂E₂–H120C from that of Cu₂Cu₂–H120C resulted in an EPR spectrum (Figure 6Cc') very similar to that obtained from the corresponding subtraction for the H46C derivatives (Figure 6Bc). This observation suggests that the geometry of Cu(II) in the zinc site is the same for Cu₂Cu₂–H46C and Cu₂Cu₂–H120C and that the imidazolate bridge is not present in either derivative. This conclusion is supported by the lack of an observable half-field EPR signal for these derivatives (Figures 7B and 7C), as was found for Cu₂Cu₂–WT (Figure 7A).

Unlike the Cu₂Cu₂ derivatives of H46C and H120C, the Cu₂Zn₂ derivatives of these mutant proteins are quite different from one another. As described above, the differences in the EPR spectra of H46C–Cu₂E₂ vs H46C–Cu₂Zn₂ are similar to those observed for WT–Cu₂E₂ vs WT–Cu₂Zn₂, suggesting that binding of Zn²⁺ to the zinc site changes the geometry of the copper site, presumably through formation of the imidazolate bridge. The EPR spectrum of Cu₂Zn₂–H120C, on the other hand, is similar to those of Cu₂Cu₂–H120C and Cu₂Cu₂–H46C, both of which have no imidazolate bridge between the bound metal ions. This result is taken as further evidence that no imidazolate bridge is present in Cu₂Zn₂–H120C.

Despite the differences between the EPR spectra of Cu₂Zn₂–H46C and Cu₂Zn₂–H120C, the spectra for both can nevertheless be readily characterized as being typical of type 2 (normal) copper proteins. Thus we can conclude that the presence of a thiolate ligand is not sufficient in itself to produce the unusual EPR spectrum with a small parallel hyperfine coupling constant nor the intense blue or blue-green color characteristic of type 1 copper proteins.²³

Electron Spin Echo Envelope Modulation (ESEEM) Spectroscopy. The electron spin echo observed for copper imidazole complexes is modulated by the nuclear spin moment of nuclei in the copper coordination sphere.^{8,24,25} The dominant interaction arises from the electron–nuclear interaction to the remote ¹⁴N of the imidazole ring of histidine ligands to the copper. The hyperfine interaction of this particular nitrogen is characterized by a nuclear hyperfine (i.e., Fermi contact) term that is approximately the same magnitude as both the nuclear quadrupole coupling and nuclear Zeeman terms (typically 1–3

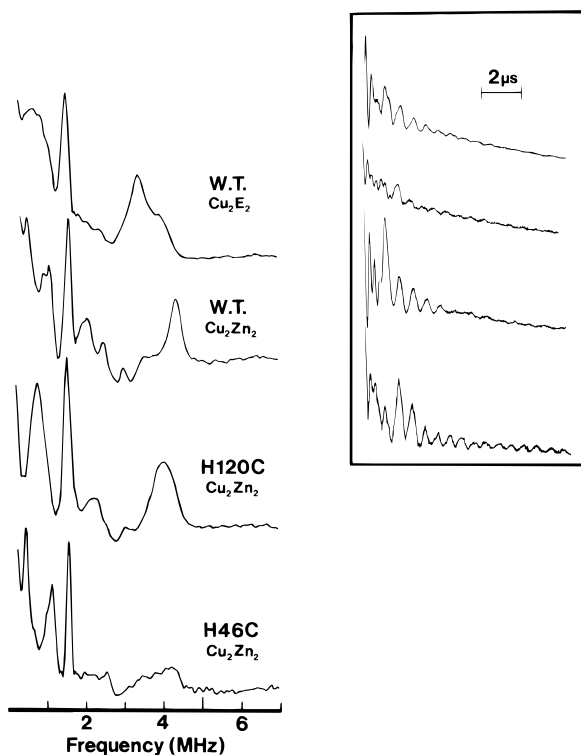


Figure 9. Electron spin echo envelope modulation (inset) and the Fourier transform spectra of the copper sites of yeast CuZnSOD derivatives recorded at g_⊥. Nuclear quadrupole transitions centered at approximately 0.7 MHz either overlap as a broad line, giving a characteristic Cu²⁺–imidazole complex type of spectrum, as in the case of WT Cu₂E₂SOD and H120C Cu₂Zn₂SOD, or are split, as in the case of WT Cu₂Zn₂SOD and H46C Cu₂Zn₂SOD. The splitting is attributed to the presence of the Cu–imidazolate–Zn bridge (see text for discussion). Operating conditions: sample concentration, 1 mM; microwave frequency, 8.7 GHz; three-pulse experiment with τ set to approximately 160 ns (twice the inverse of the proton Larmor frequency in order to suppress proton modulation): temperature, 2.4 K.

MHz). The electron spin precession of these nuclei and the resultant modulation of the echo intensity may be detected on the nanosecond time scale. Because the copper binding site of wild-type Cu₂Zn₂SOD includes four histidines, we can use the weak hyperfine interactions of the remote imidazole nitrogen as a local probe of perturbations in the copper binding site caused by the H46C and H120C mutations.

The results of three-pulse electron spin echo modulations experiments are illustrated in Figure 9. The data are collected in the time domain as a sampled echo intensity and recorded as a function of the temporal spacing between the second and third pulses;²⁴ these raw data appear in the inset. The Fourier transform spectrum of each time domain trace appears to the left. The top spectrum corresponds to the echo modulation spectrum of yeast WT Cu₂E₂SOD, and the spectrum contains characteristic features of copper imidazole complexes.²⁴ These

(23) Solomon, E. I.; Baldwin, M. J.; Lowery, M. D. *Chem. Rev.* **1992**, *92*, 521–542.

(24) (a) Mims, W. B.; Peisach, J. *J. Chem. Phys.* **1978**, *69*, 4921–4930. (b) Jiang, F.; McCracken, J.; Peisach, J. *J. Am. Chem. Soc.* **1990**, *112*, 9035–9049. (c) Dikanov, S. A.; Tsvetkov, Yu. D. *Electron Spin Echo Envelope Modulation (ESEEM) Spectroscopy*; CRC Press: Boca Raton, FL, 1992.

(25) Fee, J. A.; Peisach, J.; Mims, W. B. *J. Biol. Chem.* **1981**, *256*, 1910–14.

features include (effective) zero field quadrupole transitions, which usually appear as a pair of intense lines below 2 MHz, plus a less intense and broader double quantum (i.e. forbidden transition) line near 4 MHz. The latter is comprised of nuclear hyperfine, nuclear quadrupole, and nuclear Zeeman terms. The quadrupole transitions can be estimated from the Townes–Daily theory²⁶ of $I = 1$ quadrupole coupling in zero field, that is $\nu_{\pm} = \frac{3}{4} e^2 Qq [1 \pm \eta/3]$ and $\nu_0 = \frac{1}{2} e^2 Qq$. For the amino nitrogen of imidazole, in which the hydrogen partakes of side chain interactions (i.e., a hydrogen bond), the term η tends to be very near unity and ESEEM spectra feature a pair of quadrupole lines, the lower frequency of which tends to be slightly broader. This is what we observe for yeast WT $\text{Cu}_2\text{E}_2\text{SOD}$, namely, a sharp line at approximately 1.5 MHz and a poorly resolved broad line centered near 0.7 MHz. The low frequency feature corresponds to an overlap of the ν_- and ν_0 transitions, which is the reason for the poor resolution, since contributions from the slightly disparate nitrogen atoms overlap. Assuming that $\eta \sim 1$, the high frequency transition at 1.5 MHz corresponds to ν_+ and approximately equals $e^2 Qq$ for the remote nitrogens of imidazole ligands to the copper (i.e., His46, 48, 120, and 63).

A previous ESEEM study of bovine CuZnSOD revealed a spectrum that differs from known copper imidazole complexes: the peak ordinarily at 0.7 MHz for copper imidazole is absent and replaced by a pair of narrow lines offset above and below 0.7 MHz.²⁵ This pattern is reproduced in the spectrum of reconstituted WT yeast $\text{Cu}_2\text{Zn}_2\text{SOD}$ (Figure 9). This marked splitting of the low frequency spectral lines is ascribed to the now different quadrupole coupling parameters of the remote nitrogen of His63, which acts as a bridge between the copper and zinc ions.

Spectra obtained for the mutants H46C and H120C also differ in the manner outlined in the preceding paragraphs. The ESEEM spectrum of $\text{Cu}_2\text{Zn}_2\text{H120C}$ resembles the spectrum of copper imidazole complexes in the sense that the two low frequency lines appear at approximately 0.7 and 1.5 MHz. Conversely, the H46C ESEEM spectrum is more like that of bovine and yeast $\text{Cu}_2\text{Zn}_2\text{SOD}$ in which the intact Cu–imidazole–Zn bridge alters the features seen below 1.5 MHz. We therefore conclude from these spectra that the mutation H120C causes a breakage of the imidazole bridge whereas the mutation H46C does not.

Paramagnetic Nuclear Magnetic Resonance (NMR) Spectroscopy. Paramagnetic NMR spectroscopy has been particularly valuable in the characterization of Cu_2Co_2 derivatives of CuZnSOD , and most of the signals have been assigned.^{3,15,17,27–29} We therefore applied this technique to the Cu_2Co_2 of WT and of the H46C and H120C mutant proteins.

The NMR spectra of $\text{E}_2\text{Co}_2\text{H46C}$ (Figure 10B) and $\text{E}_2\text{Co}_2\text{H120C}$ (Figure 10C) are very similar to that of $\text{E}_2\text{Co}_2\text{WT}$ (Figure 10A), indicating that the mutations at the copper site had relatively little effect on the zinc site in the E_2Co_2 derivative. The only difference between the spectra of the WT and the copper site mutant proteins is the appearance of an extra exchangeable proton in the mutant proteins (shaded peak). Of the four ligands that coordinate to the Co(II) in the zinc site (His 63, His 71, His 80, and Asp83), there should be three exchangeable protons, one from each histidine. However, only

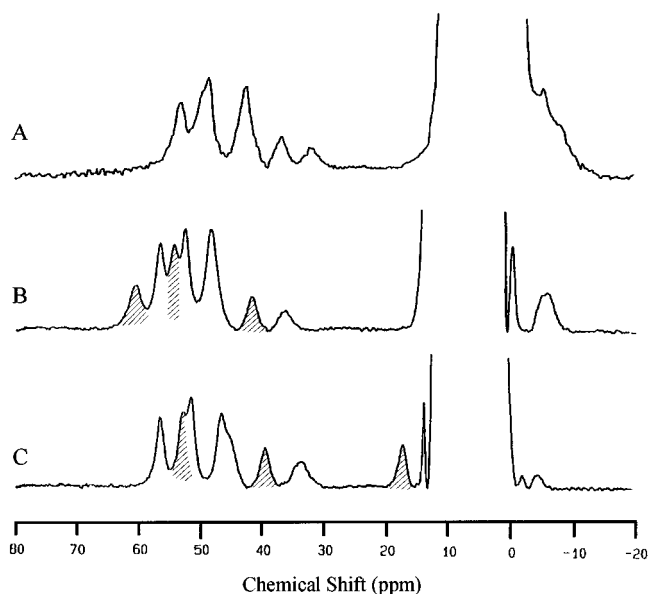


Figure 10. Isotropically shifted ^1H NMR spectra (200 MHz) of the E_2Co_2 derivatives of copper site mutant proteins H46C (spectrum B) and H120C (spectrum C) and comparison with WT (spectrum A). The shaded peaks are from exchangeable protons. Protein concentrations in subunit: H46C, 1.26 mM; H120C, 1.8 mM.

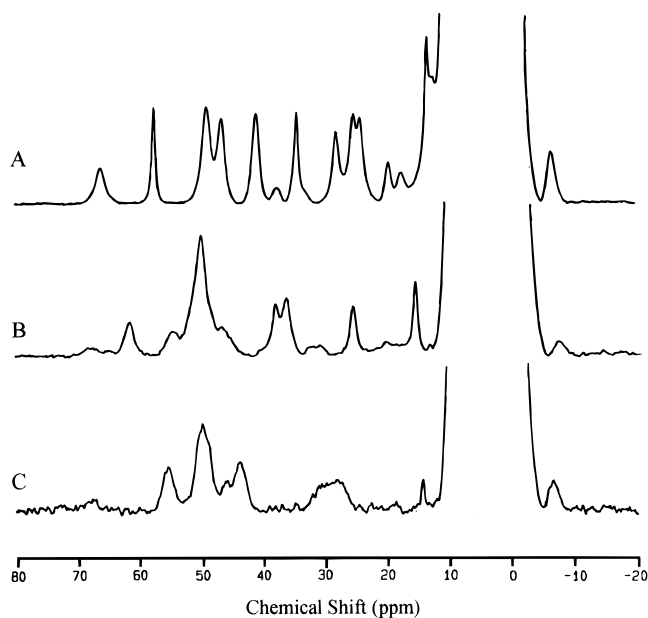


Figure 11. Isotropically shifted ^1H NMR spectra (200 MHz) of the Cu_2Co_2 derivatives of copper site mutant proteins H46C (spectrum B) and H120C (spectrum C) and comparison with WT (spectrum A). The protein concentrations are the same as in Figure 10.

two exchangeable protons could be detected with paramagnetic NMR of the WT enzyme from yeast, bovine, and human.¹⁵ This observation was interpreted to suggest that the third proton exchanges with bulk water at a rate too fast to allow it to be detected by NMR. The appearance of the third exchangeable proton in the NMR of the mutant proteins indicates that mutations at the copper site (H46C and H120C) affected the exchange rate of this proton with bulk water.

Addition of Cu^{2+} to $\text{E}_2\text{Co}_2\text{H46C}$ to form $\text{Cu}_2\text{Co}_2\text{H46C}$ caused a dramatic change in the paramagnetic NMR spectrum (Figure 11B) as it did also in the case of formation of $\text{Cu}_2\text{Co}_2\text{WT}$ from $\text{E}_2\text{Co}_2\text{WT}$ (Figure 11A), indicating that the Co(II) in the zinc site coupled with the Cu(II) in the copper site through imidazole bridge formation. The presence of the

(26) Townes, C. H.; Schawlow, A. L. *Microwave Spectroscopy*, McGraw-Hill: New York, 1955.

(27) Bertini, I.; Lanini, G.; Luchinat, C.; Messori, L.; Monnanni, R.; Scozzafava, A. *J. Am. Chem. Soc.* **1985**, *107*, 4391–4396.

(28) Banci, L.; Bertini, I.; Luchinat, C.; Piccioli, M.; Scozzafava, A.; Turano, P. *Inorg. Chem.* **1989**, *28*, 4650–4656.

(29) Banci, L.; Bertini, I.; Luchinat, C.; Piccioli, M.; Scozzafava, A. *Gazz. Chim. It.* **1993**, *123*, 95–100.

imidazolate bridge between the Cu(II) and the Co(II) ions drastically reduces the electron relaxation rates of copper(II), thus allowing for the detection of NMR signals from protons of the copper ligands.³⁰ Thus, addition of Cu²⁺ to E₂Co₂–H46C results in the appearance of new signals arising from protons on the copper ligands. However, addition of Cu²⁺ to H120C–E₂Co₂ (Figure 11C) had only a very small effect on the spectrum, similar to that seen upon addition of Ag⁺ to E₂Co₂–WT, a derivative that lacks an imidazolate bridge.³¹ In the absence of this bridge, the NMR signals of the copper ligands cannot be detected. Indeed, the spectrum in Figure 11C resembles that of E₂Co₂–H120C.

The observation of three exchangeable protons in the NMR spectrum of E₂Co₂–H120C indicates that all three histidines, i.e., His 63, His 71, and His 80, are coordinated to Co(II). The fact that the NMR spectrum is little changed when Cu²⁺ is added indicates that those three histidines remain coordinated to the Co²⁺ in Cu₂Co₂–H120C. These observations are consistent with the other spectral evidence described above that indicates that no imidazolate bridge is formed in M₂M'₂ derivatives of H120C.

Discussion

The two mutant CuZnSOD proteins described here, H46C and H120C, may be described as “type 2 (normal) copper–cysteinate proteins”.^{5–7} They are characterized by their yellow color, resulting from intense copper-to-sulfur charge transfer bands around 400 nm, and their type 2 copper protein EPR and d–d electronic absorption spectra.¹⁴ Thus they differ dramatically in their properties from type 1 (blue) copper–cysteinate proteins such as azurin and stellacyanin, which have characteristic intense sulfur-to-copper charge transfer electronic absorption bands at longer wavelengths and distinctive EPR properties, with small values for A_{||}.^{8,23} In fact, early successes in synthesizing stable copper–thiolate model complexes produced coordination complexes with spectroscopic properties characteristic of type 2 rather than type 1 copper–cysteinate proteins.^{32,33} Only relatively recently have well-characterized copper–thiolate model complexes with type 1 properties been achieved.³³ The essential feature of such complexes and of naturally occurring³⁴ and engineered^{8,35,36} type 1 copper proteins is a Cu(II) center that consists of a trigonal N₂S site. By contrast, type 2 copper–cysteinate site geometries appear in each case to be four- or five-coordinate and to have geometries tending toward tetragonal rather than trigonal. Apparently the geometry of the Cu(II) center is the primary determinant of type 1 vs type 2 properties for copper–cysteinate proteins.

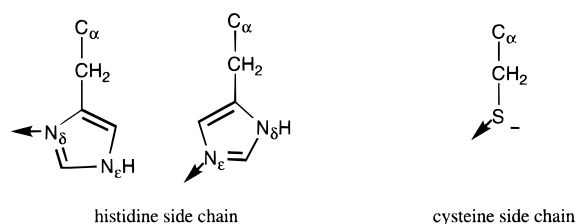
In an earlier report,⁸ we described the successful reengineering of the tetrahedral zinc site of yeast CuZnSOD into a type 1 copper center by the replacing one of the histidines with cysteine and Zn(II) with Cu(II). In the present work, we have introduced cysteines in place of histidines in the roughly tetragonal copper site and produced type 2 cysteinate proteins. In all of these cases, the overall properties of the mutant proteins are remarkably similar to those of the wild type protein, and the changes

produced by the mutations appear to be localized to the site of each mutation. In other words, even though the mutated residues are those that provide ligands to the metal ions, the changes in the geometries of the metal sites as a result of each mutation appear to be minimal.

In the case of H46C CuZnSOD, each derivative that contains Cu(II) in the copper site has a sulfur-to-copper charge transfer transition around 370 nm. Apart from that new spectroscopic feature, however, the spectroscopic properties of the metal-substituted derivatives of H46C are remarkably similar to those of the analogous derivatives of the wild-type protein. Moreover, it appears that the imidazolate bridge between the copper and zinc sites that is characteristic of the wild-type protein is retained in H46C, with the one exception that the imidazolate bridge does not appear to be present in the Cu₂Cu₂ derivative (see above). The remarkable preservation of native-like structure in H46C CuZnSOD is particularly interesting since His46, a copper-site ligand, and His71, a zinc-site ligand, are both hydrogen bonded to the carboxylate group of Asp124 in the wild-type CuZnSOD proteins.^{37–40} Thus Asp124 provides a secondary bridge between the two metal-binding sites in addition to the primary bridge provided by the imidazolate ligand from His63. Mutation of Asp124 to Gly has been shown in the human protein to lower drastically the affinity of the zinc site for metal ions,³⁹ suggesting that this secondary bridge plays an important role in stabilizing the zinc site. It is therefore surprising and interesting to us that the His46Cys mutation, which removes His46 from the secondary bridge, has relatively little effect on the metal-binding affinities of the protein.

For the H120C mutation, once again each derivative that contains Cu(II) in the copper site has a sulfur-to-copper charge transfer transition, in this case, around 400 nm, and once again, many of the spectroscopic properties of the metal-substituted derivatives are similar to those of the analogous derivatives of the wild-type protein. However, the distinctive spectroscopic characteristics that originate from the presence of the imidazolate bridge which are observed for WT and H46C are absent in H120C. Thus the paramagnetic NMR and the d–d region of the visible spectra of Cu₂Co₂–H120C as well as the ESEEM spectra of Cu₂Zn₂–H120C are dramatically different from those of the analogous WT and H46C derivatives and provide strong evidence that the imidazolate bridge is not present.

It is important to note that the cysteinyl side chain is significantly shorter than the histidyl side chain, and some accommodation, either local or long-range, from the protein structure is therefore likely to be required in order for Cys to replace His as a copper ligand. There are three bonds from the backbone C_α to the N_δ of His, four bonds to the N_ε of His, but only two bonds to the S of Cys.



(30) Banci, L.; Bertini, I.; Luchinat, C. *Nuclear and Electron Relaxation*; VCH: Weinheim, Germany, 1991.

(31) Ming, L.-J.; Valentine, J. S. *J. Am. Chem. Soc.* **1990**, *112*, 4256–4264.

(32) Hughey, J. L.; Fawcett, T. G.; Rudich, S. M.; Lalancette, R. A.; Potenza, J. A.; Schugar, H. J. *J. Am. Chem. Soc.* **1979**, *101*, 2617–2623.

(33) Kitajima, N. *Adv. Inorg. Chem.* **1992**, *39*, 1–77.

(34) Adman, E. T. *Adv. Protein Chem.* **1991**, *42*, 145–197.

(35) Maret, W.; Dietrich, H.; Ruf, H.-H.; Zeppezauer, M. *J. Inorg. Biochem.* **1980**, *12*, 241–252.

(36) Brader, M. L.; Borchardt, D.; Dunn, M. F. *J. Am. Chem. Soc.* **1992**, *114*, 4480–4486.

(37) Ogihara, N.; Hart, J.; Eisenberg, D.; Valentine, J. S. unpublished results.

(38) Parge, H. E.; Hallewell, R. A.; Tainer, J. A. *Proc. Natl. Acad. Sci. U.S.A.* **1992**, *89*, 6109–6113.

(39) Banci, L.; Bertini, I.; Cabelli, D. E.; Hallewell, R. A.; Tung, J. W.; Viezzoli, M. S. *Eur. J. Biochem.* **1991**, *196*, 123–128.

(40) Tainer, J. A.; Getzoff, E. D.; Beem, K. M.; Richardson, J. S.; Richardson, D. C. *J. Mol. Biol.* **1982**, *160*, 181–217.

Inspection of the X-ray crystal structures of the CuZnSOD metal binding site shows that the imidazole of His46 binds to Cu(II) via N_δ, whereas the imidazole ring of His120 binds via N_ε (see Figure 1).^{37,38,40} The similarity in the metal-binding and spectroscopic properties of H46C CuZnSOD and wild type suggests that whatever accommodation is required for cysteine to coordinate to the copper in this mutant is accomplished with little movement from other parts of the protein, i.e., a local accommodation. In the case of H120C, however, there appears to be competition between Cys120 and the ligand *trans* to it, i.e., His63, the bridging imidazolate, for copper ligation, and a long-range accommodation of the protein structure and/or a movement of the metal ion is required in order for the cysteine to coordinate. Among the biological ligand donors such as nitrogen, oxygen, and sulfur, the cysteine sulfur is known to be a particularly favorable ligand for copper(II). Our results indicate that a configuration in which Cu(II) is bound to Cys120, and not to the potential bridging His63, is more favorable. Thus Cys120 coordinates to the copper, and the imidazolate bridge does not form for Cu₂M₂-H120C.

Preliminary studies indicate that substitution of cysteine for histidine in the metal-binding sites significantly alters both the electron transfer properties and superoxide dismutase activities of CuZnSOD. Further investigations of this nature are in progress.

Acknowledgment. Helpful discussions with Drs. Li-June Ming, John Tainer, and Edward I. Solomon are gratefully acknowledged. We also thank Dr. David Goodin for use of the Bruker 300D EPR spectrometer at the Scripps Research Institute. This work was supported by grants from PHS (GM-28222 to J.S.V.; GM-40168 and RR-02583 to J.P.), and a New Faculty Grant from Loyola Marymount University (J.A.R.). Y.L. also acknowledges a Hortense Fishbaugh Memorial Scholarship, a Phi Beta Kappa Alumni Scholarship Award, and a Product Research Corporation Prize for Excellence in Research.

IC9513189